Korean J. Chem. Eng., **29**(7), 891-902 (2012)
DOI: 10.1007/s11814-011-0269-0

Hydraulic characteristics analysis of an anaerobic rotatory biological contactor (AnRBC) using tracer experiments and response surface methodology (RSM)

Yadollah Mansouri*, Ali Akbar Zinatizadeh,†, Parviz Mohammadi***, Mohsen Irandoust****, Aazam Akhbari*****,******, and Reza Davoodi******

*Young Researchers Club, Ilam Branch, Islamic Azad University, Ilam, Iran
**Water and Wastewater Research Center (WWRC), Department of Applied Chemistry, Faculty of Chemistry, Razi University, Kermanshah, Iran
***Department of Environmental Health Engineering, Kermanshah Health Research Center (KHRC), Kermanshah University of Medical Sciences, Kermanshah, Iran
****Department of Analytical Chemistry, Faculty of Chemistry, Razi University, Kermanshah, Iran
*****Sama Technical and Vocatinal Training College, Islamic Azad University, Kermanshah Branch, Kermanshah, Iran
******Kermanshah Water and Wastewater Company, Kermanshah, Iran
(*Received 19 June 2011 • accepted 15 October*)

Abstract−The hydraulic characteristic of an anaerobic rotating biological contactor (AnRBC) were studied by changing two important hydraulic factors effective in the treatment performance: the hydraulic retention time (τ) and rotational disk velocity (ω). The reactor hydraulic performance was analyzed by studying hydraulic residence time distributions (RTD) obtained from tracer (Rhodamine B) experiments. The experiments were conducted based on a central composite face-centered design (CCFD) and analyzed using response surface methodology (RSM). The region of exploration for the process was taken as the area enclosed by τ (60, 90 and 120 min) and ω (0.8 and 16 rpm) boundaries. Four dependent parameters, deviation from ideal retention time ($\Delta\tau$), dead volume percentage and dispersion indexes (Morrill dispersion index (MDI) and dispersion number (d)), were computed as response. The maximum modeled $\Delta\tau$ and dead volume percentage was 43.03 min and 37.51% at τ and ω 120 min and 0 rpm, respectively. While, the minimum predicted responses (2.57 min and 8.08%) were obtained at τ and ω 60 min and 16 rpm, respectively. The interaction showed that disk rotational velocity and hydraulic retention time played an important role in MDI in the reactor. The AnRBC hydraulic regime was classified as moderate and high dispersion (d=0.09 to 0.253). As a result, in addition to the factors studied, the reactor geometry showed significant effect on the hydraulic regime.

Key words: Anaerobic Rotatory Biological Contactor, Hydraulic Characteristics, Tracer Experiment, Response Surface Methodology

INTRODUCTION

The hydraulic behavior in biological reactors is of fundamental importance for the efficiency of wastewater treatment processes. Examples of hydraulic phenomena with adverse impacts on the bioreactors performance include short circuiting streams and dead volumes. The unfavorable hydraulic situations in the bioreactors may cause lower process performance and thus higher residual concentrations in the treated water. This may be particularly significant in high loaded bioreactors and anaerobic RBC reactors [1,2]. Owing to a lack of appreciation for the hydraulics of reactors, many of the treatment plants that have been built do not perform hydraulically as designed. Comparison of actual hydraulic characteristics of a reactor measured using tracers, to the expected theoretical response can be used to assess the degree to which the ideal design has been achieved [2,3].

Anaerobic rotating biological contactors (AnRBCs) offer an alternative treatment technology to the conventional anaerobic digester. Because of the widespread use of RBCs in recent years, and because the reactor hydraulics directly affects the treatment performance, determination of hydraulic characteristic is of great importance. Poor hydraulic conditions reduce the HRT and effective volume, resulting in lower removal efficiencies of the bioreactor. The presence of a good design model for the RBC reactor is a useful tool for describing and predicting the RBC hydraulic regime [4-6].

There are several examples of tracer tests being used to indicate the presence of short circuiting streams and dead volume in different reactors. Hydraulic characterization is performed by a retention time distribution (RTD) curve [7-11]. Not many tracer studies have been done on the hydraulic characteristics of the RBC reactor, but a few quantitative models have been proposed [12-16]. In all these models, there is no common agreement on whether an RBC behaves as a plug-flow or a completely mixed reactor. Various indexes have been used to describe the mixing and hydraulic flow pattern in the different operational units. These are Morrill (MDI), Peclet, dispersion (d) numbers etc [1-3]. Non-ideal flow models such as the tank-in-series (TIS) model and dispersion plug flow (DPF) model are used to describe the hydraulic flow pattern of an anaerobic baffled reactor (ABR) [17].

Today, improvements in computer and computational technology and the development of a new generation of highly efficient computer programs like computational fluid dynamic (CFD) analysis

†To whom correspondence should be addressed.
E-mail: aliazinatiz@yahoo.com, zinatizadeh@razi.ac.ir

have made it possible to show the inside dynamic flow situation in structures such as clarifiers and activated sludge reactors [18,19]. Response surface methodology (RSM) is a collection of statistical and mathematical techniques useful for the process modeling and optimizing. This methodology is more practical compared to the other approaches as it arises from experimental methodology, which includes interactive effects among the variables and, eventually, it depicts the overall effects of the parameters on the process [20].

In an earlier work published elsewhere [21], we found that low hydraulic retention time (τ) and disk rotational velocity (ω) had an adverse impact on the process performance. Hence, in the present study, in order to explore the best operational conditions achieving a high hydraulic performance in an anaerobic RBC, the interactions among two effective variables (τ, ω) as well as their direct impacts on the hydraulic regime of the AnRBC were investigated. The responses (deviation from ideal retention time ($\Delta\tau$), volume of dead space and dispersion indexes (MDI and d)) were determined using the data obtained from the tracer experiments, and the hydraulic characteristics were analyzed and modeled by RSM.

MATERIALS AND METHODS

1. Bioreactor Configuration

The AnRBC reactor made of Plexiglas is illustrated in Fig. 1. The trough size of the reactor was 15.5 cm in total length and 14.5 cm in width, having a semi-circular bottom in cross-sectional view. The reactor had a 2,890 ml as working volume; 12 fully immersed disks with 12 cm in diameter which were connected via a stainless steel shaft to a motor and rotated at 0-16 rpm parallel to the direction of wastewater flow. The opening of each of the disks was 1 cm and the distance between disks was about 1 cm. The influent flow rate was regulated by a peristaltic pump. The reactor was cleaned at the end of each run.

2. Tracer Experiments Procedure

A unique technique for studying the flow pattern in a reactor is analysis of tracer-response profiles. In this study, Rhodamine B was used as a tracer, because this substance is not absorbed on or reacted with the exposed reactor surface, and can be detected at very low concentration with a spectrophotometer. In each run, the desired flow of tap water into the reactor was introduced by peristaltic pump according to the experiments that were designed by Design Expert software (Stat-Ease Inc., version 6.0.7) with two variables, hydraulic retention time (τ) and disk rotational velocity (ω). The samples were taken from the effluent after each interval time.

The Design Expert software is a windows-compatible software which provides efficient design of experiments (DOEs) for the identification of vital factors that affect the process and uses RSM to determine optimal operational conditions. The results can be obtained as 3D presentations for visualization and also as contours to appreciate the effect of system variables on responses. In this experiment, 2.5 ml of a concentrated solution of Rhodamine B (0.0123 M) was instantly introduced into the inlet of the reactor. Effluent

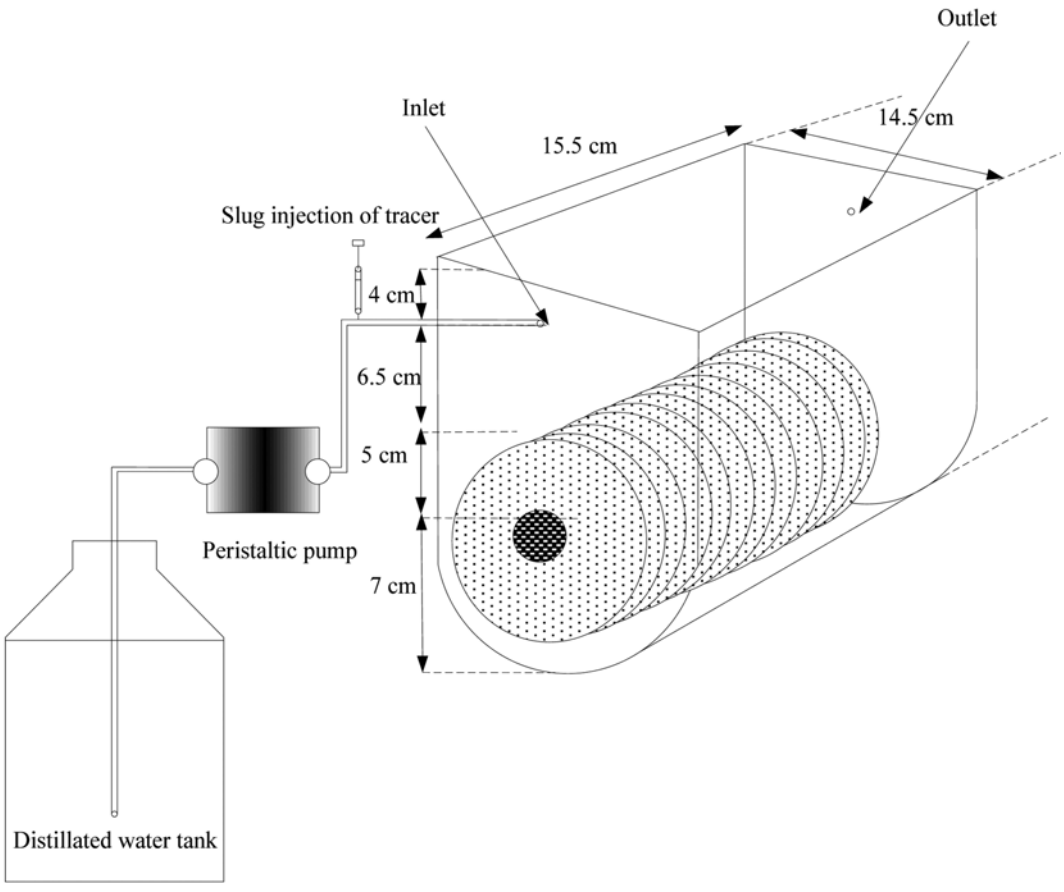

Fig. 1. Experimental set up.

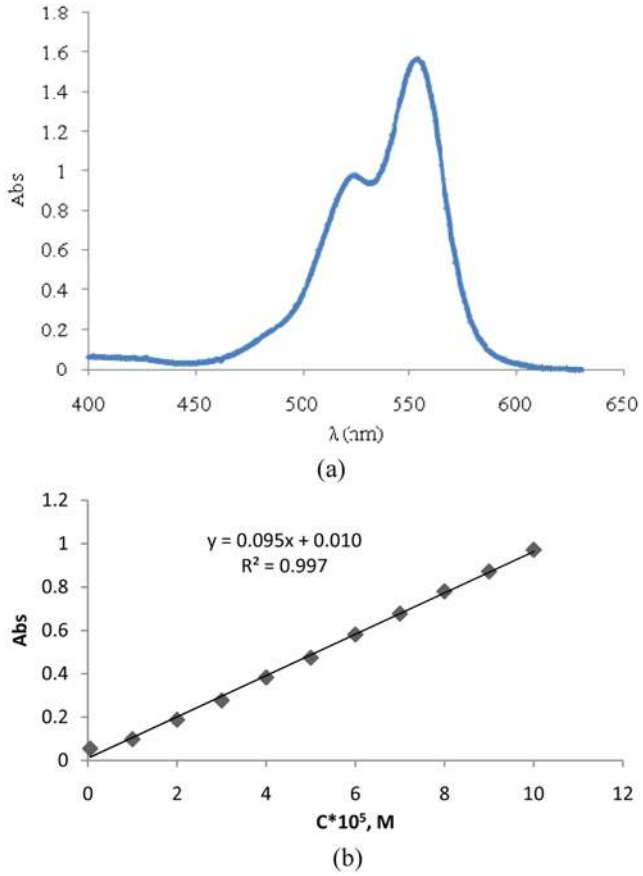

Fig. 2. (a) Absorption spectra of 2×10^{-4} M Rhodamine B, (b) Calibration graph for determination of Rhodamine B at its respective absorbance (λ_{max}=554 nm).

samples were collected immediately after the observation of the tracer in the effluent at every 5 min or at lesser time intervals and tested by spectrophotometer. The operation was continued until no tracer was detected for at least 2 or 3 times of HRT.

Absorption spectra of Rhodamine B (2×10^{-4} M) were obtained in the range of 400-630 nm (Fig. 2(a)). Maximum absorption appeared at 554 nm at room temperature with UV-visible spectrophotometer (Agilent 8453, Germany). This maximum absorption was used throughout the experiments. Fig. 2(b) shows the calibration curve obtained for Rhodamine B at its respective absorbance λ_{max} (554 nm) with correlation coefficient value of 0.999.

3. Experimental Design

Three important hydraulic factors that influence the treatment performance of a RBC reactor are hydraulic retention time (τ), disk rotational velocity (ω) and degree of submergence. The latter variable is eliminated for anaerobic RBC as the disks were fully submerged in the system. In this study, τ and ω were therefore chosen as the independent and most critical operating factors on the hydraulic regime. The region of exploration for hydraulic regime in the AnRBC reactor was decided as the area enclosed by τ(60, 120 min) and ω (0, 16 rpm) boundaries (Table 1). Selection of the range of the ω was based on the results obtained from the earlier studies [22,23]. The operating conditions as well as their standard deviations are presented in Table 2, indicative of good agreement between the designed and actual values.

Table 1. Experimental range and levels of the independent variables

Variables	Range and levels		
	−1	0	1
Hydraulic retention time (τ), min	60	90	120
Disk rotational velocity (ω), rpm	0	8	16

The statistical method of factorial design of experiments (DOE) eliminates systematic errors with an estimate of the experimental error and minimizes the number of the experiments [24]. In this study, as no reaction occurs and both variables and responses are inherently hydraulic parameters, the face-centered design with the minimum levels was proposed. In the face-centered design, the axial points occur at the center of each face of the factorial space, rather than outside the faces as in the case of a spherical region, so $\alpha=\pm1$. This design requires three levels of each factor. In addition, another reason for selecting face-centered design in this study was that the effects of the variables on the responses in the values between the range studied (−1 to +1) had not shown any unknown curvature in the literatures as well as in our preliminary study, meaning that it does not affect the obtained trend. Therefore, the RSM used in the present study was a central composite face-centered design (CCFD) involving two different factors, τ and ω.

The hydraulic regime of the AnRBC reactor was assessed based on the full face-centered CCD experimental plan (Table 3). The design consisted of 2^k factorial points augmented by 2k axial points and a center point where k is the number of variables. The two operating variables were considered at three levels namely, low (−1), central (0) and high (1). Accordingly, 13 experiments were conducted with nine experiments organized in a factorial design (including four factorial points, four axial points and one center point) and the

Table 2. Standard deviation of operating conditions applied in this study

Factor	Designed value in DOE	Range of measured value during experiment	Standard deviation
Hydraulic retention time (τ), min	60	60.84	±0.092
	90	91.75	±0.148
	120	122.46	±0.113
Disk rotational velocity (ω), rpm	0	0	±0.0
	8	8	±0.0
	16	16	±0.0

Table 3. Experimental conditions and results of central composite design

Run	Variables		Responses				
	Factor 1	Factor 2	Deviation from ideal retention time	MDI	Dead volume percentage	Dispersion number (d)	Peclet number
	Hydraulic retention time (τ)	Disk rotational velocity (ω)					
	min	rpm	min	-	%	-	-
1	60	16	3.61	64	07.29	0.23	3.9
2	90	16	22.2	51	17.12	0.19	4.2
3	120	16	31.31	30	28.20	0.13	4.9
4	60	0	19.12	26	33.46	0.14	7.1
5	90	8	13.57	26	17.12	0.16	5.2
6	90	8	9.56	29	14.30	0.17	5.1
7	120	0	43.18	36	37.86	0.10	10.0
8	60	8	9.58	44	17.79	0.18	4.9
9	90	8	17.57	23	21.12	0.15	5.4
10	90	8	15	35	24.00	0.16	4.9
11	120	8	26.51	26	24.30	0.13	7.7
12	90	8	13	20	19.00	0.14	5.4
13	90	0	32.43	56	37.67	0.13	7.7

remaining four involving the replication of the central point to get good estimate of experimental error. Repetition experiments were carried out after other experiments followed by order of runs designed by DOE as shown in Table 3.

To do a comprehensive analysis on the hydraulic regime, four dependent parameters were calculated as response. These parameters were deviation from ideal retention time ($\Delta\tau$), volume of dead space, Morrill dispersion index (MDI) and dispersion number (d). The parameters were determined by the following relationships.

$$E(t)=\frac{C(t)}{\int_0^\infty C(t)dt} \tag{1}$$

$$\bar{t}=\sum(t)E(t)\Delta t \tag{2}$$

$$\Delta\tau=\tau-\bar{t} \tag{3}$$

$$\text{Volume of dead space, } \%=\left(1-\frac{\bar{t}}{\tau}\right)100 \tag{4}$$

$$MDI=\frac{P_{90}}{P_{10}} \tag{5}$$

$$F(t)=\int_0^{t'} E(t)dt \tag{6}$$

$$\sigma_c^2=\frac{\int_0^\infty t^2C(t)dt}{\int_0^\infty C(t)dt}-(\bar{t}_c)^2 \tag{7}$$

$$\sigma_\theta^2=\frac{\sigma_c^2}{\tau^2}=2\frac{D}{uL}+8\left(\frac{D}{uL}\right)^2 \tag{8}$$

$$p_e=\frac{uL}{D} \tag{9}$$

$$d=\frac{D}{uL} \tag{10}$$

where, C(t) is tracer concentration at time t, mg/*l*; $\bar{t}$ is mean residence time, min; E(t) is residence time distribution function; $\Delta\tau$ is deviation from ideal retention time, min; MDI as a measure of the dispersion is Morrill dispersion index; P_{90} is 90 percentile value from log-probability plot, %; P_{10} is 10 percentile value from log-probability plot, % and F(t) is cumulative residence time distribution function.

After the experiments were conducted, the coefficients of the polynomial model were calculated using the following equation [25]:

$$Y=\beta_0+\beta_iX_i+\beta_jX_j+\beta_{ii}X_i^2+\beta_{jj}X_j^2+\beta_{ij}X_iX_j+\ldots \tag{11}$$

Where i and j are the linear and quadratic coefficients, respectively, and β is the regression coefficient. Model terms were selected or rejected based on the P-value with 95% confidence level. The results were completely analyzed using analysis of variance (ANOVA) by Design Expert software. Three-dimensional plots and their respective contour plots were obtained based on the effect of the levels of the two factors. From these three-dimensional plots, the simultaneous interaction of the two factors on the responses was studied. The experimental conditions and results are shown in Table 3.

RESULTS AND DISCUSSION

1. Tracer Study

The hydraulic performance of the AnRBC reactor was analyzed by studying water flow patterns or hydraulic residence time distributions (RTD) obtained from the tracer experiments. Fig. 3(a)-(c) presents the modeled and experimental data curves of the tracer concentration versus time distribution at different τ (60, 90 and 120 min) and ω (0, 8 and 16 rpm). It is clear from the figure that increase in τ resulted in an increase in deviation from ideal flow pattern, while

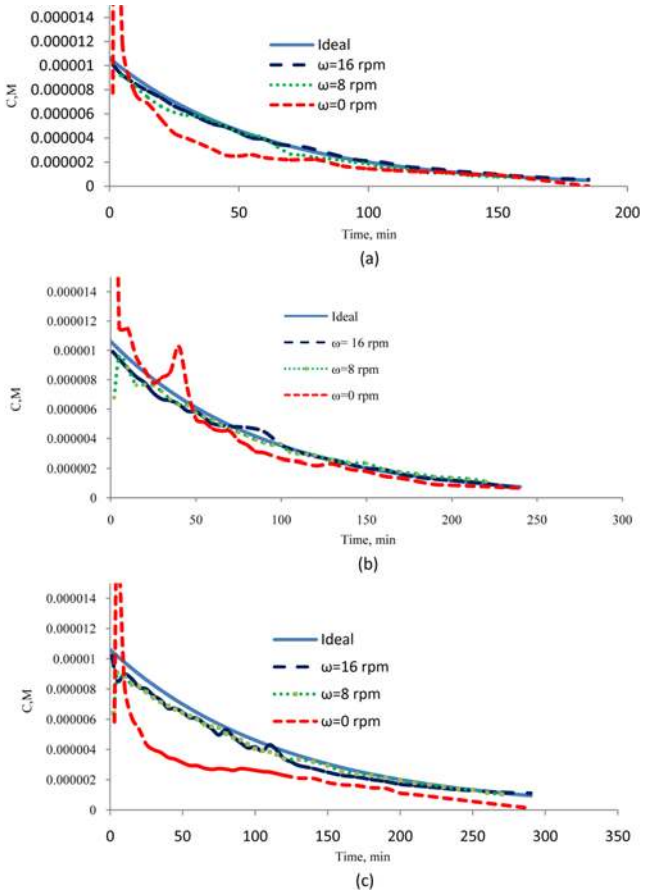

Fig. 3. Mathematical and empirical curves of tracer concentration time distribution for (a) τ=60 min, (b) τ=90 min, (c) τ= 120 min.

an increase in disk rotational velocity caused a decrease in the deviation. Comparing the results presented in the figures, it can be seen that the maximum deviation was obtained at τ and ω, respectively, 120 min and 0 rpm, whereas, the minimum value of the deviation was obtained at minimum τ (60 min) and ω (0 rpm). As depicted in Fig. 3, high volume of the tracer arrives at the outlet before mixing with bulk of the liquid in the reactor as disk rotational velocity equals zero. It was due to the short-cut phenomenon that occurred which originated from the reactor geometry, inlet and outlet design and inadequate mixing. From the viewpoint of hydraulic operation, the values of τ and ω, respectively, 60 min and 16 rpm were advisable since they corresponded to the lowest deviation detected.

In general, the RTD curve shows a discrepancy between the mean residence time and the theoretical residence time. However, it is possible that stagnate hydraulic zones exist near the inlet or between the disk, where the tracer can be trapped and slowly released. It must be noted that, in this reactor, the liquid volume between the disks is 60% of the total liquid volume. Furthermore, the small space between the disks (1 cm) can hinder the tracer flow, resulting in high dead volumes for some conditions of τ.

2. Hydraulic Performance Analysis

2-1. Statistical Analysis

The ANOVA results for all responses are summarized in Table 4. As various responses were investigated in this study, different degree polynomial models were used for data fitting (Table 4). To quantify the curvature effects, the data from the experimental results were fitted to higher degree polynomial equations (i.e., quadratic model). In the Design Expert software, the response data were analyzed by default. The model terms in the equations are those remained after the elimination of insignificant variables and their interactions. Based on the statistical analysis, the models were highly significant with very low probability values (from 0.019<0.0001). It is shown that the model terms of independent variables were significant at 99% confidence level. The square of correlation coefficient for each response was computed as the coefficient of determination (R^2). It showed high significant regression at 95% confidence level. The value of the adjusted determination coefficient (adjusted R^2) was also high to prove the high significance of the model [25].

The model's adequacy was tested through lack-of-fit F-tests [26]. The lack of fit results were not statistically significant as the P values were found to be greater than 0.05. Adequate precision is a measure of the range in predicted response relative to its associated error or, in other words, a signal to noise ratio. Its desired value is 4 or more (26). The value was found to be desirable for all models. Simultaneously, low values of the coefficient of variation (CV) (13.39-17.75%) indicated good precision and reliability of the experiments as suggested by [25,28]. Detailed analysis of the models is presented in the following sections.

2-2. Deviation from Ideal Retention Time ($\Delta\tau$)

Deviation from the ideal retention time ($\Delta\tau$) can be caused by channeling and/or recycling of fluid, short circuiting, creation of stagnant regions in the vessel, and etc. In short circuiting, a portion of the flow that enters the reactor during a given time period arrives at the outlet before the bulk of the flow that enters the reactor during the same time period arrives. The non ideal flow (short circuiting) can be caused by density currents (due to temperature difference), wind-driven circulation patterns, inadequate mixing and poor

Table 4. ANOVA results for the equations of the design expert 6.0.6 for studied responses

Response	The models selected to describe the responses	Probability	R^2	Adj. R^2	Adeq. precision	SD	CV	PRESS	Probability for lack of fit
Deviation from ideal retention time	Modified quadratic model	<0.0001	0.927	0.903	20.67	3.45	17.75	228.38	0.315
MDI	Modified quadratic model	<0.019	0.651	0.536	7.65	9.39	26.20	2705.80	0.103
Dead volume percentage	Modified quadratic model	<0.0001	0.925	0.888	15.38	4.08	13.39	189.97	0.815
Dispersion number	Modified quadratic model	<0.0001	0.97	0.96	33.34	8.7	4.81	1.97	0.377

R^2: determination coefficient, Adj. R^2: adjusted R^2, Adeq. Precision: adequate precision, SD: standard deviation, CV: coefficient of variation, PRESS: predicted residual error sum of squares

design. Ultimately, the incomplete use of the reactor volume due to the above reasons can result in increased $\Delta\tau$ and reduced treatment performance.

The ANOVA values for $\Delta\tau$ at different conditions are shown in Table 4. The Following equation shows the dependency of the response to the variables studied based on coded values:

$$\Delta\tau, \text{min} = +21.16 + 11.42\ A - 7.94\ B \quad (12)$$

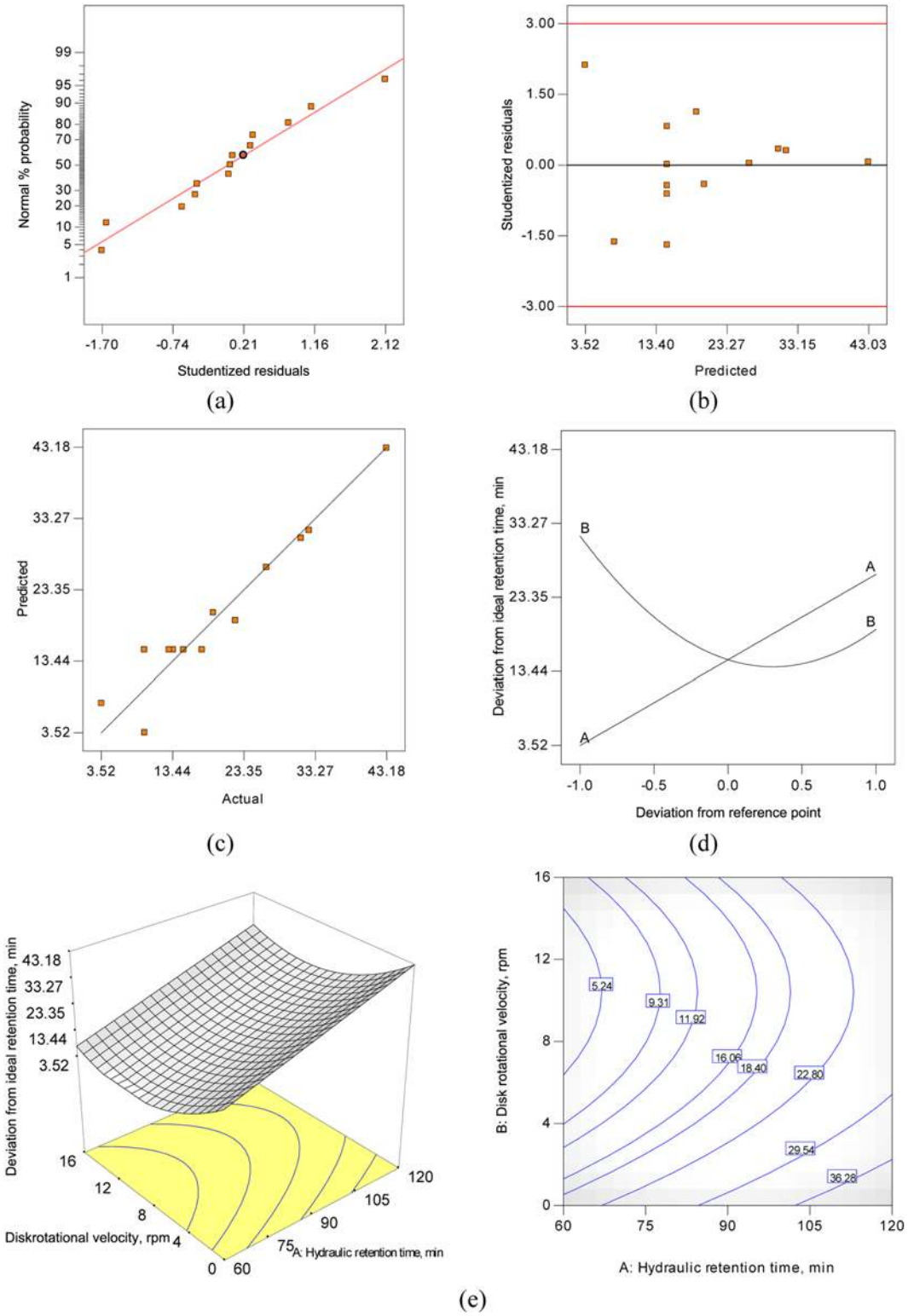

Fig. 4. (a) Normal probability plot of residual for deviation from ideal retention time ($\Delta\tau$), (b) Residual versus predicted Plot for deviation from ideal retention time ($\Delta\tau$), (c) Predicted vs. actual values plot for deviation from ideal retention time ($\Delta\tau$), (d) Perturbation plot for deviation from ideal retention time ($\Delta\tau$), (e) 3D and contour plots with respect to τ and ω for deviation from ideal retention time ($\Delta\tau$).

From the equation, the main effect of A and B was significant model terms. ANOVA results of these quadratic models presented in Table 4 indicate that the above equation could be used to navigate the design space. Fig. 4(a) displays the normal probability of the residuals, to verify whether the standard deviations between the actual and the predicted responses values do follow the normal distribution. The general impression from the Fig. 4(a) reveals that the underlying errors were distributed normally as the residuals fall near to a straight line, and thus, there is no severe indication of non-normality of the experimental results.

The plots of the residuals versus predicted response are presented in Fig. 4(b). The general impression is that the plot should be a random scatter, suggesting that the variance of original observations is constant for all values of the response. If the variance of the response depends on the mean level of the response, then this plot often exhibits a funnel-shaped pattern [26,29,30]. This is also an indication that there was no need for transformation of the response variable. As depicted in the Fig. 4(b) all points of experimental runs were scattered randomly within the constant range of residuals across the graph, i.e., within the horizontal lines at point of ±3.0. This implies that the model proposed is adequate and the constant variance assumption was confirmed.

The actual and the predicted plot for $\Delta\tau$ are shown in Fig. 4(c). In the figure the values of R^2 and R^2adj were evaluated as 0.93 and 0.90, respectively. The perturbation plot (Fig. 4(d)) shows the comparative effects of all variables on the response. It is clear from this figure that the response was very sensitive to both variables (τ and ω).

Fig. 4(e) depicts 3D and contour plots for $\Delta\tau$ with respect to the two variables (τ and ω) in the studied design space. From the results, the two factors were found to be influential in the response as confirmed in the perturbation plot (Fig. 4(e)). As noted in Fig. 4(d) and (e), increasing in the ô resulted in an increase in the response, while the reverse effect was caused by increasing the disk rotational velocity. This is proved in the model with positive and negative coefficients. From Fig. 4(e), an increase in ω from 0 to 8 rpm caused a remarkable decrease in $\Delta\tau$, whereas further increase in ω did not show any significant effect on the response. It was attributed to the relatively high volume of the liquid over the disks that creates dead space, so that the energy supplied by the disks rotation was not sufficient for eliminating the effects of the spaces. The maximum value of the modeled $\Delta\tau$ was 43.03 min at τ and ω, 120 min and 0 rpm, respectively. Whereas, the minimum predicted response (2.57 min) was obtained at τ and ω 60 min and 16 rpm, respectively. High value of $\Delta\tau$ at low disk rotational velocity (as shown in the Fig. 4(e)) resulted in inadequate mixing as well as poor design of this reactor. Without sufficient energy input, portions of the reactor contents may not mix with the incoming water; also, because of the poor design of the reactor (close and opposite inlet and outlet), dead zones develop within the reactor that will not mix with the incoming water or short circuiting occurs.

2-3. Dead Volume Percentage

To elucidate the $\Delta\tau$, the dead zone volume was also studied as a response. Dead space can be categorized into hydraulic dead space and biological dead space. Hydraulic dead space is a function of flow rate and the number of disks in the reactor, while biological dead space is a function of the biomass concentration and activity. However, the hydraulic dead space is the major contributor to the dead space of AnRBC, especially in treating low strength wastewater because the biological dead space resulting from gas flow velocity and diffusion of the tracer into biofilm is neglected (due to the tin biofilm formed on the discs).

ANOVA results for dead volume are shown in Table 4. As it is noted in the table, a quadratic model was fitted with the experimental data. The quadratic model shows that the main effect of τ (A), ω (B), two-level interaction (AB) and second order effects of B^2 are significant model terms in the response. Other model term, A^2, is not significant (with a probability value larger than 0.05). Therefore, this model term was excluded from the study to improve the model. The following regression equation is the empirical model in terms of the coded factors for dead volume percentage.

$$\text{Dead volume, \%} = +19.66 + 5.30A - 9.40\,B + 7.27\,B^2 + 4.13\,AB \quad (13)$$

The major diagnostic plots in Figs. 5(a)-(d) are used to determine the residual analysis of response surface design, ensuring that the statistical assumptions fit the analysis data. The results obtained from diagnostic plots and ANOVA results showed that values of dead volume percentage from the model and the actual experimental data were in good agreement. The predicted versus actual plot for the response is in Fig. 5(c), which shows that the actual values are distributed relatively close to the straight line (y=x). The perturbation plot (Fig. 5(d)) shows the comparative effects of τ and ω on the response. From the results, more significant factors on dead volume were found to be disk rotational velocity (with similar trend as demonstrated in Fig. 4(d) and e for $\Delta\tau$). Fig. 5(e) presents 3D and contour plots of the modified quadratic model for variation in the volume of dead space, as a function of τ (A) and ω (B). In the figure the response increased upon increasing the τ and decreasing the ω. The worst condition was obtained for τ=120 min and ω=0, which is explained by the inadequate mixing and low flow rate. For the experiments of hydraulic retention time 60 and 90 min in ω=0 the detected dead volume was also very high. The maximum response observed was 37.86% at τ and ω of 2 h and 1 rpm, respectively. While, the minimum predicted response (8.08%) was obtained at τ and ω of 1 h and 16 rpm, respectively.

2-4. Dispersion Indexes

2-4-1. Morrill Dispersion Index (MDI)

One important factor that indicates the type of the reactor (complete mix or plug-flow) is the Morrill dispersion index (MDI). MDI can be used as a diagnostic tool for ascertaining the features of flow patterns in reactors. These include the possibilities of bypassing and/or regions of stagnant fluid (i.e., dead space). A ratio of 90 to 10 percent values from the cumulative tracer curve (Fig. 3) could be used as a measure of the dispersion index. The value for an ideal plug-flow reactor is 1.0 and about 22 and more for complete-mix reactors. MDI was computed for different operational conditions studied.

The ANOVA results for MDI are shown in Table 4. From the analysis, A, AB and B^2 are significant model terms. Insignificant model terms were found to be B and A^2 that were excluded from the model to improve the model.

$$\text{MDI} = +29.03 - 7.03A + 14.77B^2 - 11.00AB \quad (14)$$

The predicted versus actual plot for MDI is shown in Fig. 6. While the R^2 value of the modified quadratic model (R^2=0.65) is not as

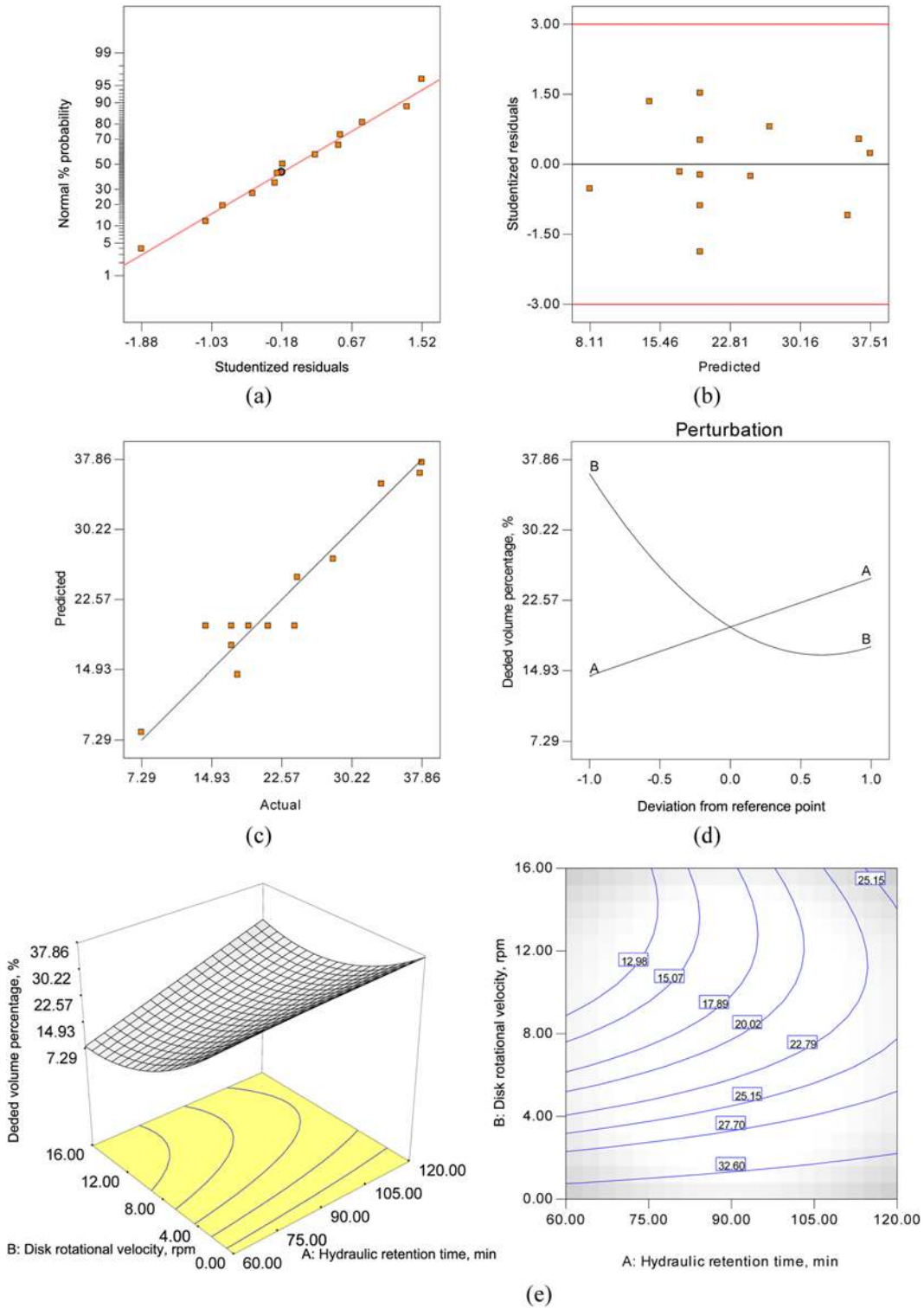

Fig. 5. (a) Normal probability plot of residual for Dead volume percentage, (b) Residual versus predicted Plot for Dead volume percentage, (c) Predicted vs. actual values plot for Dead volume percentage, (d) Perturbation plot for Dead volume percentage, (e) 3D and contour plots with respect to τ and ω for Dead volume percentage.

high as that of the models for the other responses, it nevertheless, shows a reasonable degree of correlation between the parameters (Fig. 6). Fig. 7 shows the response surface and contour plots of the quadratic model for MDI with respect to τ (A) and ω (B) within the design space. As can be seen in the Fig. 7, the most significant factor on MDI was determined to be ω. A reverse impact of increasing disk rotational velocity on MDI was observed as the variable increased (Fig. 7). At low τ (corresponding to high flow rate), an increase in disk rotational velocity (from 0 to 8) caused a decrease in the response. Whereas, at higher ω (from 8 to 16) an increase in

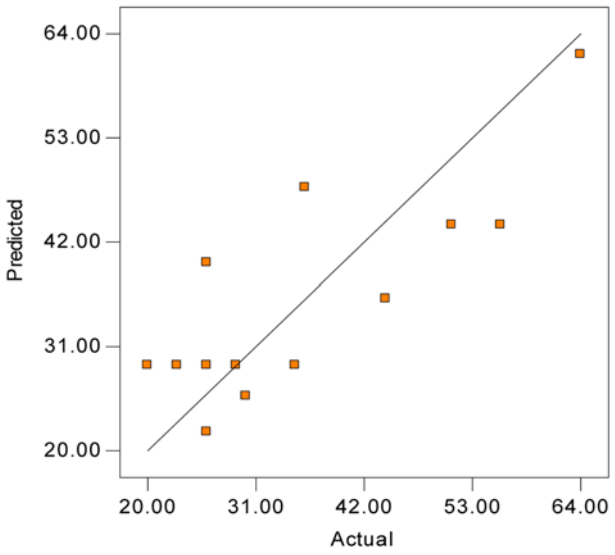

Fig. 6. Predicted vs. actual values plot for MDI.

the variable increased the response.

Decreasing in τ and increasing in ω together leads the hydraulic regime to complete mixing, which is identified by the higher values of MDI. From the results shown in Fig. 7, the aforementioned principle is confirmed except for the data obtained at the conditions with no mechanical mixing (ω=0 rpm). The high value of the MDI in the lower ω was not a sign of the high value of mixing and dispersion. This was because of the short-cut phenomenon that resulted from the poor reactor geometry and inlet and outlet design. As can be seen in Fig. 1, inlet and outlet are against each other with 6.5 cm away from the disks, providing about one-third of the reactor volume in the upper part where adequate mixing is not supplied. The poor design of the inlet and outlet develops a dead zone within the reactor. The reason is justified by the normalized residence time distribution curves shown in the Fig. 7.

To elucidate the residence time distribution of the fluid in the reactor, the E(t) and F(t) curves have been shown in corners of Fig. 7. From the E(t) curve, the initial peak at ω=0 (τ=60 and 120 min) clearly indicates a short circuiting stream. Also, as shown in Eq. (6), the F(t) curve is the integral of the E(t) curve, while the E(t) curve represents the amount of the tracer that has remained in the reactor for less than the time t. As can be observed, E(t) and F(t) show higher initial values at the lowest ω compared to the values at the higher ω. So that, at τ=60 min and ω=0, 48% of the fluid had a residence time of less than 5 minutes, 41% between 5 and 60 minutes and 11% more than 60 minutes. While these values were obtained 8.34, 57.11 and 34.5%, respectively, at τ=60 min and ω=16 rpm. For τ=120 and ω=0, the values were 16.05% with τ less than 10 minutes, 57.53% between 10 and 120 minutes and 26.42% more than 120 minutes. Whereas, for τ=120 and ω=16, the values were obtained, respectively, 9.1, 63.97 and 26.93%. The interaction showed that disk rotational velocity and τ played an important role in MDI in the reactor. The maximum MDI was found to be 61.83 at τ and ω of 60 min and 16 rpm respectively.

2-4-2. Dispersion Number

Another important response describing the hydraulic behavior

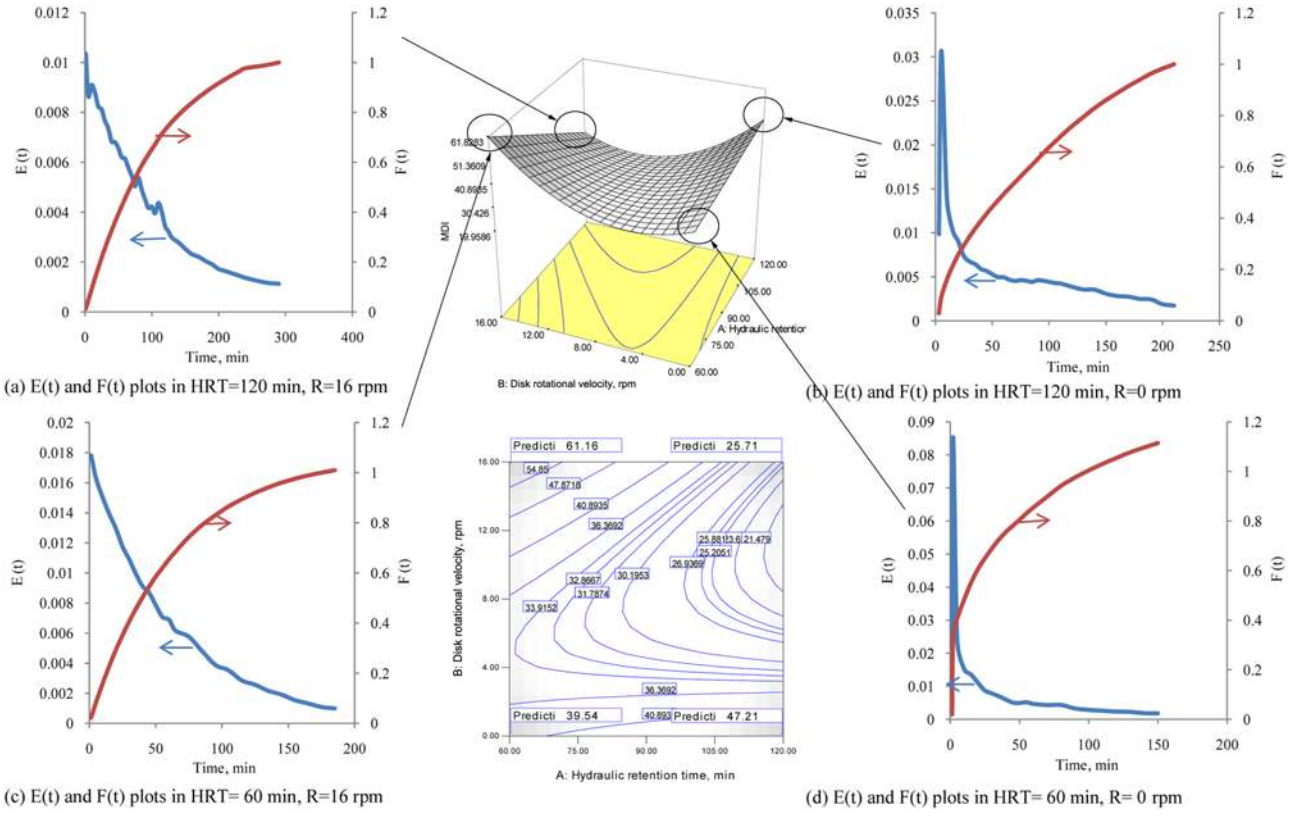

Fig. 7. Response surface and counter plots for MDI with respect to τ and ω.

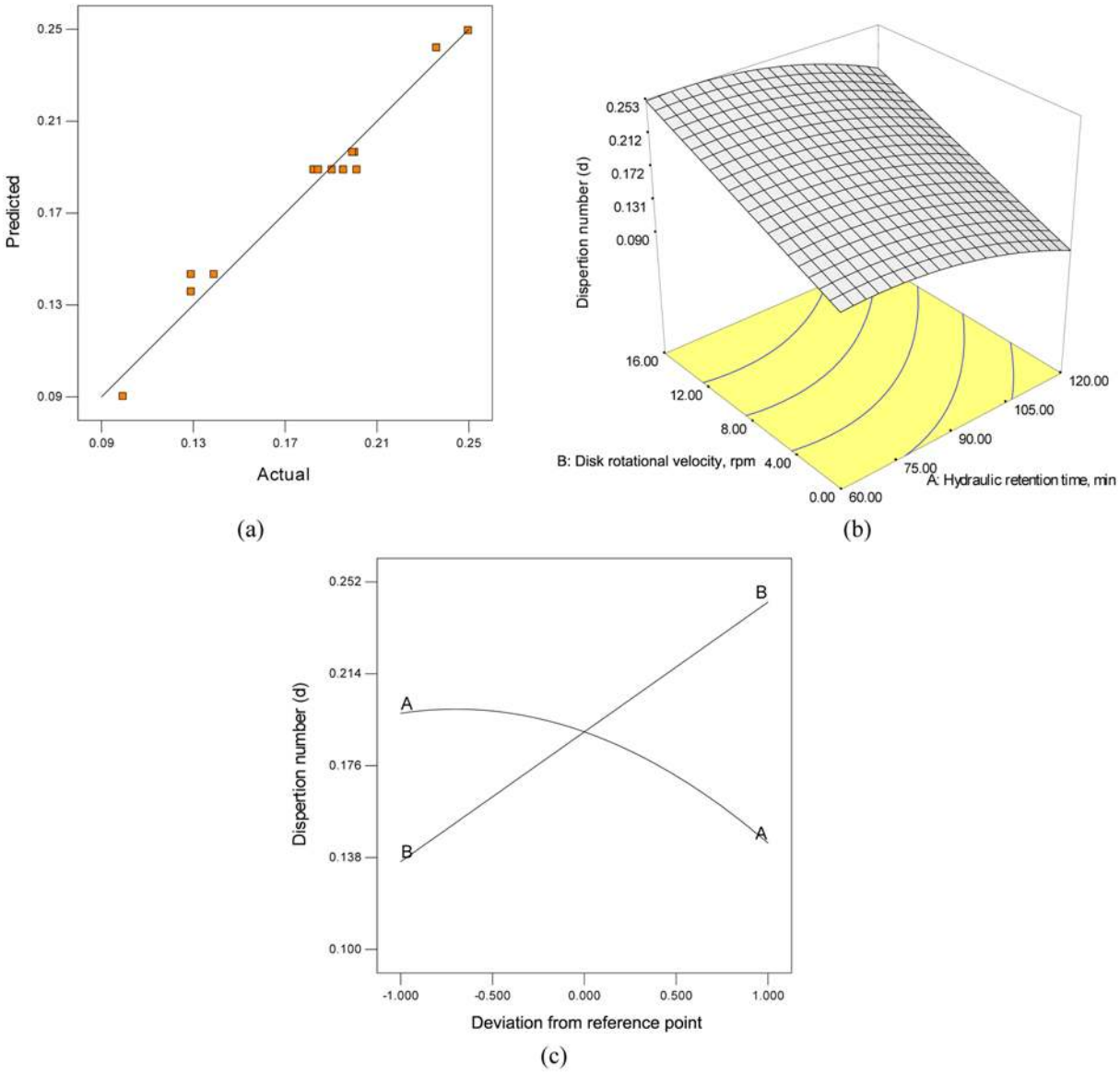

Fig. 8. (a) Predicted vs. actual values plot for dispersion number, (b) 3D plot with respect to τ and ω for Dispersion number, (c) Perturbation plot for dispersion number.

of the AnRBC is the dispersion, which is a measure of the degree of mixing in the bioreactor. As the dispersion increases, the concentration of a certain pollutant decreases and thus leads to higher removal efficiency. A complementary measure of the dispersion is the dispersion number, which is defined as the inverted Peclet number (Eq. (9) and Table 3). To get a meaningful interpretation of the flow pattern in the AnRBC reactor, the values of dispersion number in the different conditions as a response were calculated and displayed in Table 3.

The predicted versus actual plot for the response (Fig. 8(a)) shows that the actual values are distributed close to the straight line (y=x). From the ANOVA results (Table 4), A, B and A^2 are significant model terms. Insignificant model terms, which have limited influence, such as AB and B^2, were excluded from the study to improve the model. The following regression equation is the empirical model in terms of coded factors for dispersion number (d):

$$\text{Dispersion number (d)} = +0.19 - 0.027A + 0.054 * B - 0.019A^2 \quad (15)$$

The effects of τ and ω on the dispersion number are shown in Fig. 8(b). The most significant factor effective in the response was determined to be disk rotational velocity (ω). Increase in ω from 0 to 15 min/h resulted in an increase in dispersion number with a main order effect, while with increase in τ the response was decreased. The perturbation plot shown in Fig. 8(c) demonstrates the comparative effects of τ and ω on the response. An increasing linear slope in ω and decreasing curvature of τ shows that the response was sensitive to these two process variables with different effects.

The maximum and minimum dispersion number was obtained 0.253 and 0.09 at τ and ω of 60 min, 16 rpm and 120 min, 0 rpm, respectively. However, for practical purposes, the following dispersion values can be used to assess the degree of axial dispersion in wastewater treatment facilities [3].

No dispersion d=0 (ideal plug flow)
low dispersion d≤0.05
Moderate dispersion d=0.05-0.025
High dispersion d≥0.25

Based on the computed values of the dispersion number (0.09 to 0.253) and above discussion, the AnRBC hydraulic regime is classified as moderate and high dispersion. At low disk rotational velocity and higher hydraulic retention time, the values of d were observed to be low. In contrast, at high disk rotational speeds, high d was obtained. Hence, it may be stated that, in a majority of flow situations, an AnRBC reactor behaves more like a complete mix regime with axial dispersion rather than being a plug flow one.

CONCLUSION

The hydraulic characteristics of the AnRBC reactor at various levels of hydraulic retention time (τ) and disk rotational velocity (ω) were constructively investigated. This study showed that in addition to the factors studied, reactor geometry had a significant effect on the hydraulic regime. Improving the reactor design (modifying inlet and outlet structure, eliminating the dead volume, etc.) can avoid high energy consumption supplied by the disk rotation or influent flow rate that is strongly advised for scale-up stage. However, the following salient points were obtained.

- τ and ω were found to be influential for the deviation from ideal retention time ($\Delta\tau$). Increasing τ resulted an increase in $\Delta\tau$; while the reverse effect was caused by increasing the disk rotational velocity. The volume of dead space increased upon increasing the τ and decreasing the ω.
- Based on the computed values of the dispersion number (0.09 to 0.253), the AnRBC hydraulic regime is classified as moderate and high dispersion. In the majority of flow situations, the AnRBC reactor behaved more like a complete mix regime with axial dispersion rather than being a plug flow one.
- Most significant factor on MDI was ω. At low HRTs (corresponding to high flow rate), an increase in disk rotational velocity (from 0 to 8) caused a decrease in the response. While at higher rpm (from 8 to 16), an increase in the variable increased the response. The maximum MDI was found to be 61.83 at τ and ω of 60 min and 16 rpm, respectively.

ACKNOWLEDGEMENT

The financial support provided by Kermanshah Water and Wastewater Company is gratefully acknowledged. The authors acknowledge the laboratory equipment provided by the Water and Power Industry Institute for Applied and Scientific Higher Education (Mojtama-e-gharb), Kermanshah that has resulted in this article. The authors also wish to thank Mrs S. Kiani for her assistance (Technical Assistant of Water and Wastewater Laboratory).

NOMENCLATURE

AnRBC : anaerobic rotating biological contactor
CCD : face-centered design
CCFD : central composite face-centered design
CFD : computational fluid dynamic
C(t) : tracer concentration at time t [mg/*l*]
CV : coefficient of variation
D : coefficient of axial dispersion [m^2/s]
d : dispersion number
DoE : design of experiment
E(t) : residence time distribution function
F(t) : cumulative residence time distribution function
i : linear coefficient
j : quadratic coefficient
k : number of variables
L : characteristic length [m]
MDI : morrill dispersion index
P_{90} : 90 percentile value from log-probability plot [%]
P_{10} : 10 percentile value from log-probability plot [%]
P_e : peclet number
RSM : response surface methodology
RTD : retention time distribution
u : fluid velocity [m/s]
$\Delta\tau$: deviation from ideal retention time [min]
β : regression coefficient
$\bar{t}$: mean residence time [min]
σ_c^2 : variance of normalized tracer response [s^2]
σ_θ^2 : variance derived from C curve [s^2]
ω : rotational disk velocity
τ : hydraulic retention time

REFERENCES

1. O. Levenspiel, *Chemical reactor engineering*, 2nd Ed., Wiley, New York (2000).
2. H. Fogler Scott, *Elements of chemical reaction engineering*, 3rd Ed., Prentice Hall PTR (2001).
3. Metcalf & Eddy, *Wastewater engineering*, 4th Ed., McGraw Hill, New York (2003).
4. T. Yamaguch, I M.T., shida Suzuki, *J. Process Biochem.*, **35**, 403 (1999).
5. F. Kargi and S. Eker, *J. Enzyme Microb. Technol.*, **32**, 464 (2003).
6. G. D. Najafpour, A. A. L. Zinatizadeh and L. K. Lee, *J. Biochem. Eng.*, **30**, 297 (2006).
7. H. Bode and C. Seyfried, *J. Water Sci. Technol.*, **17**, 197 (1984).
8. B. Newell, J. Bailey, A. Islam, L. Hopkins and P. Lant, *J. Water Sci. Technol.*, **37**, 43 (1998).
9. S. C. Williams and J. Beresford, *J. Water Sci. Technol.*, **38** 55 (1998).
10. L. J. Burrows, A. J. Stokes, A. D. West and C. F. Martin, *J. Water Res.*, **33**, 367 (1999).
11. A. D. Martin, *J. Chem. Eng. Sci.*, **55**, 5907 (2000).
12. B. H. Kornegay and J. F. Andrews, *J. WPCF*, 460 (1968).
13. J. H. Clark, E. M. Moneg and T. Asano, *J. WPCF*, 896 (1978).
14. Y. C. Wu and E. D. Smith, *J. Environ. Eng. Div.*, (Proc. ASCE) 108 (1982).
15. K. P. Hsueh, O. J. Hao and Y. C. Wu, *J. WPCF*, **63**, 67 (1991).
16. G. Banerjee, *J. Water Res.*, **31**, 2500 (1997).
17. Y. Saratha1, T. Koottatep and A. Morel, *J. Environ. Scien.*, **22**, 1319 (2010).
18. A. B. Karama, O. O. Onyejekwe, C. J. Brouckaert and C. A. Buckley, *J. Water Sci. Technol.*, **39**, 329 (1999).
19. J. Zhang, P. M. Huck and W. B. Anderson, *Optimization of a full-*

scale ozone disinfection process based on computational fluid dynamics analysis, in 11th gothenburg symposium, Chemical Water and Wastewater Treatment VIII. Orlando, Florida, USA (2004).
20. D. Bas and B. I. H. Oyaci, *J. Food Eng*., **78**, 836 (2007).
21. A. Akhbari, A. A. Zinatizadeh, P. Mohammadi, M. Irandoust and Y. Mansouri, *J. Chem. Eng*., **168,** 269 (2011).
22. L. D. Palma, C. Merli, M. Paris and E. Petrucci, *J. Bioresour*., (2003).
23. A. Tawfik, A. Klapwijk, F. El-Gohary and G. Lettinga, *J. Biochem. Eng*., **25**, 89 (2005).
24. R. Kuehl, Design of Experiments: *Statistical principles of research design and analysis*, 2nd Ed., C.A: Duxbury Press (2000).
25. A. I. Khuri and J. A. Cornell, *Response surfaces: Design and analyses*, 2nd Ed., Marcel Dekker, New York (1996).
26. D. C. Montgomery, *Design and analysis of experiments*, 3rd Ed., Wiley, NewYork (1991).
27. R. L. Mason, R. F. Gunst and J. L. Hess, *Statistical design and analysis of experiments*, *eighth applications to engineering and science*, 2nd Ed., Wiley, New York (2003).
28. A. L. Ahmad, S. Ismail and S. Bhatia, *J. Environ. Sci. Technol*., **39**, 2828 (2005).
29. R. H. Myers and D. C. Montgomery, *Response surface methodology: Process and product optimization using designed experiments*, 2nd Ed., Wiley, New York (2002).
30. D. C. Montgomery, *Design and analysis of experiments*, 4th Ed., Wiley, New York (1996).